

# Gamma-Ray De-Excitation of the Low Levels of $F^{18}$

J. A. KUEHNER, E. ALMQVIST, AND D. A. BROMLEY

*Atomic Energy of Canada Limited, Chalk River Laboratories, Chalk River, Ontario, Canada*

(Received December 16, 1960)

The reaction  $O^{16}(He^3, p)F^{18}$  has been employed to study the de-excitation gamma-ray branching of levels in  $F^{18}$  up to about 3 Mev using  $p\gamma$  coincidence techniques. These measurements have been shown to be in reasonable agreement with tentative level identifications, 0 Mev ( $1+$ ), 0.94 Mev ( $3+$ ), 1.04 Mev ( $0+$ ,  $T=1$ ), 1.12 Mev ( $5+$ ), 1.70 Mev ( $1+$ ), 2.10 Mev ( $2+$ ), 2.53 Mev ( $3+$ ), and 3.06 or 3.13 Mev unresolved ( $2+$ ,  $T=1$ ), based on the intermediate-coupling shell-model predictions of Elliott and Flowers and of Redlich. An additional level at 1.08 Mev, which may arise from core excitation, is shown likely to have spin zero. It is suggested that the predicted energies need to be reduced by a factor of 0.6 and that the  $T=1$  levels require shifting with respect to the  $T=0$  levels to bring them into agreement with experiment. It has not been found possible to obtain an adequate fit to the  $F^{18}$  level spectrum presented in terms of a rotational collective model. The data may, however, be qualitatively in accord with an alpha- $N^{14}$  cluster model interpretation. An example of the isotopic spin selection rule inhibiting  $\Delta T=0$   $M1$  transitions in self-conjugate nuclei has been found.

## A. INTRODUCTION

UNTIL recently, very little was known regarding the level structure of  $F^{18}$ . However, interest has increased in the last few years, in part at least, as a result of theoretical studies of the mass-18 system.<sup>1-5</sup> Several experimental investigations<sup>6-9</sup> have established the excitations of the levels for the first few Mev excitation in  $F^{18}$ , but, as yet, very little has been reported regarding the characteristics of these levels.

Measurements on the angular distributions of deuterons<sup>10</sup> and of tritons<sup>11,12</sup> from the inverse stripping reactions  $F^{19}(p, d)F^{18}$  and  $F^{19}(d, t)F^{18}$ , which might have been expected to yield level parities in the residual nucleus, and on the  $Ne^{20}(d, \alpha)F^{18}$  reaction,<sup>13</sup> which should identify the  $T=0$  levels in  $F^{18}$ , have been hindered either by low intensity or inadequate energy resolution, with the result that these measurements have yielded little unambiguous information concerning assignments. This is particularly true of the recently recognized<sup>6</sup> quartet of levels near one-Mev excitation in  $F^{18}$ .

More recently, measurements on the gamma radiation<sup>14,15</sup> following the beta decay of  $Ne^{18}$  and on the relative feeding<sup>9</sup> of the residual  $F^{18}$  states in  $Ne^{20}(d, \alpha)F^{18}$  have established the level at 1.04 Mev as the  $0+ T=1$  analog of the ground state of  $O^{18}$ .

Measurements of the lifetime<sup>16</sup> and of the internal conversion coefficient<sup>17</sup> of the gamma-ray transition between the  $F^{18}$  levels at 1.12 and 0.94 Mev strongly suggest an  $E2$  transition and are consistent with these two levels being the  $5+$  and  $3+$  members of a predicted triad including the  $1+$  ground state.

These assignments are consistent with a double stripping interpretation of some proton angular distributions in the  $O^{16}(He^3, p)F^{18}$  reaction<sup>18</sup> and in the  $O^{16}(t, p)O^{18}$  reaction<sup>19</sup> and are also consistent with measurements described below.

An experimental investigation of the low levels of  $F^{18}$ , via a study of the reaction  $O^{16}(He^3, p)F^{18}$ , is reported herein. Preliminary reports on these measurements have been reported previously.<sup>20</sup> These measurements include  $p\gamma$  coincidence studies leading to gamma-ray de-excitation branching ratios for the levels up to and including that at 3.13 Mev. Some selected  $p\gamma$  angular correlation measurements have been made in

<sup>1</sup> M. G. Redlich, Phys. Rev. **95**, 448 (1954).

<sup>2</sup> J. P. Elliott and B. H. Flowers, *Proceedings of the Glasgow Conference on Nuclear and Meson Physics* (Pergamon Press, New York, 1955), p. 77.

<sup>3</sup> J. P. Elliott and B. H. Flowers, Proc. Roy. Soc. (London) **A229**, 536 (1955).

<sup>4</sup> M. G. Redlich, Phys. Rev. **110**, 468 (1958).

<sup>5</sup> J. P. Elliott, Proc. Roy. Soc. (London) **A245**, 128 (1958), and Proc. Roy. Soc. (London) **A245**, 562 (1958).

<sup>6</sup> J. A. Kuehner, E. Almqvist, and D. A. Bromley, Phys. Rev. Letters **1**, 260 (1958).

<sup>7</sup> T. E. Young, G. C. Phillips, R. R. Spencer, and D. A. A. S. N. Rao, Phys. Rev. **116**, 962 (1959).

<sup>8</sup> S. Hinds and R. Middleton, Proc. Phys. Soc. (London) **A73**, 721 (1959).

<sup>9</sup> J. M. Freeman (private communication).

<sup>10</sup> E. F. Bennett, Bull. Am. Phys. Soc. **3**, 26 (1958); Princeton University thesis, 1958 (unpublished); Phys. Rev. Letters **6**, 208 (1961).

<sup>11</sup> F. A. El-Bedewi and I. Hussein, Proc. Phys. Soc. (London) **A70**, 233 (1957).

<sup>12</sup> N. A. Vlasov, S. P. Kalinin, A. A. Ogloblin, and V. I. Chuev, J. Exptl Theoret Phys. (U.S.S.R.) **37**, 1187 (1960) [translation: Soviet Phys.-JETP **37**(10), 844 (1960)].

<sup>13</sup> R. Middleton and C. T. Tai, Proc. Phys. Soc. (London) **A64**, 801 (1951).

<sup>14</sup> J. W. Butler and K. L. Dunning, Bull. Am. Phys. Soc. **5**, 101 (1960), and private communication.

<sup>15</sup> D. Eccleshall and M. J. L. Yates, Proc. Phys. Soc. (London) **77**, 93 (1961).

<sup>16</sup> K. W. Allen, D. Eccleshall, and M. J. L. Yates, Proc. Phys. Soc. (London) **A74**, 660 (1959).

<sup>17</sup> T. A. Rabson, T. W. Bonner, R. Castillo-Bahena, M. V. Harlow, H. P. Haenni, and W. A. Ranken, Nuclear Phys. (to be published).

<sup>18</sup> S. Hinds and R. Middleton, Proc. Phys. Soc. (London) **A74**, 762 (1959).

<sup>19</sup> A. A. Jaffe, I. J. Taylor, and P. D. Forsyth, Proc. Phys. Soc. (London) **A75**, 940 (1960).

<sup>20</sup> J. A. Kuehner, E. Almqvist, and D. A. Bromley, Bull. Am. Phys. Soc. **3**, 27 (1958); D. A. Bromley, J. A. Kuehner, and E. Almqvist, *Proceedings of the Rehovoth Conference on Nuclear Structure*, edited by H. J. Lipkin (North-Holland Publishing Company, Amsterdam, 1959), p. 70; E. Almqvist, D. A. Bromley, and J. A. Kuehner, *Proceedings of the 1958 Accelerator Conference* (High Voltage Engineering Corporation, Burlington, Massachusetts, 1958), p. A14.

addition to  $\gamma\gamma$  coincidence measurements. Excitation curves for protons detected at  $90^\circ$  have been measured for incident energies from 2.1 to 3.2 Mev.

The reactions competing with  $O^{16}(He^3,p)F^{18}$  ( $Q = 2.034$  Mev) are  $O^{16}(He^3,\alpha)O^{15}$  ( $Q = 4.976$  Mev) and  $O^{16}(He^3,\gamma)Ne^{19}$  ( $Q = 8.416$  Mev). The yield of gamma radiation from the latter of these is so small<sup>21</sup> as to be undetectable with the apparatus used. In general, no difficulty was encountered in separating the alpha-particle groups from the proton groups.

## B. EXPERIMENTAL EQUIPMENT

The experimental equipment used in this work was conventional and in large part has been described previously. Three types of spectrometer were used to detect and to measure the energies of protons from the reaction. These consisted of a CsI(Tl) crystal spectrometer with low resolution and high efficiency,<sup>22</sup> a Frisch-gridded ionization chamber,<sup>21</sup> and a high-resolution but low-efficiency Kellogg-type magnetic analyzer.<sup>23</sup> In general, the CsI crystal spectrometer was used in  $p\gamma$  coincidence measurements while the ionization chamber and magnet were used for direct measurements. Two gamma-ray spectrometers comprising 5-in. diameter by 4-in. long NaI(Tl) crystals<sup>24</sup> were mounted on an angular distribution table, allowing their rotation in a horizontal plane containing the beam and the target. The target and CsI crystal mounts used in the coincidence measurements have been described previously.<sup>22</sup> The CsI detector was mounted at  $90^\circ$  to the incident beam axis either vertically above the target or in the horizontal plane containing the target. In addition, it could be mounted above the beam at  $145^\circ$  to its axis.

For the measurements using the Kellogg magnet or the ionization chamber, a continuously variable angular distribution chamber<sup>25</sup> was employed allowing detection at angles of  $-30^\circ$  through  $0^\circ$  to  $+144^\circ$  with respect to the beam axis.

The CsI crystals were covered by 0.0004-inch Al to stop scattered beam and the ionization chamber used a window of 1.3 mg/cm<sup>2</sup> mica.

The counters were used in conjunction with combined "fast-slow" coincidence and pulse amplitude analysis circuits. The coincidence resolving time,  $2\tau$ , was  $4 \times 10^{-8}$  sec. Pulse-height spectra of gamma rays coincident with gamma-ray or proton pulses of a selected amplitude range were displayed on a 100-channel pulse-height analyzer.

The preparation of the targets used in these meas-

urements has been described previously.<sup>21</sup> Thick targets of molybdenum trioxide ( $MoO_3$ ) on molybdenum backings and thin targets of aluminum oxide ( $Al_2O_3$ ) either on aluminum backings or self-supporting were used. The thicknesses of these  $Al_2O_3$  films were in the range 250 Å to 4000 Å. The thinnest of these represents 10 kev energy loss for a 2.5-Mev  $He^3$  ion.

## C. RESULTS

### 1. Proton Spectra

Figure 1(a) is the pulse-height spectrum obtained using a CsI crystal to detect charged particles emerging from the target at  $90^\circ$  to a 2.95-Mev  $He^3$  beam. The system gain was such that the high-energy tail of the ground-state proton group,  $P_0$ , fell above the upper limit of the pulse-height analyzer. The counts at the low pulse-height end of the scale were mainly due to low-energy radiations such as  $\beta$  rays and bremsstrahlung from the target. This contribution disappears when a requirement of coincidence with gamma radiation is imposed [see Fig. 1(b)]. However, in Fig. 1(b) the shape of the spectrum in the region of  $P_{8,9}$  is considerably distorted due to the small pulse-height cutoff of the coincidence circuit.

Figure 2 shows the results of a measurement on the proton groups using the magnetic analyzer set for a

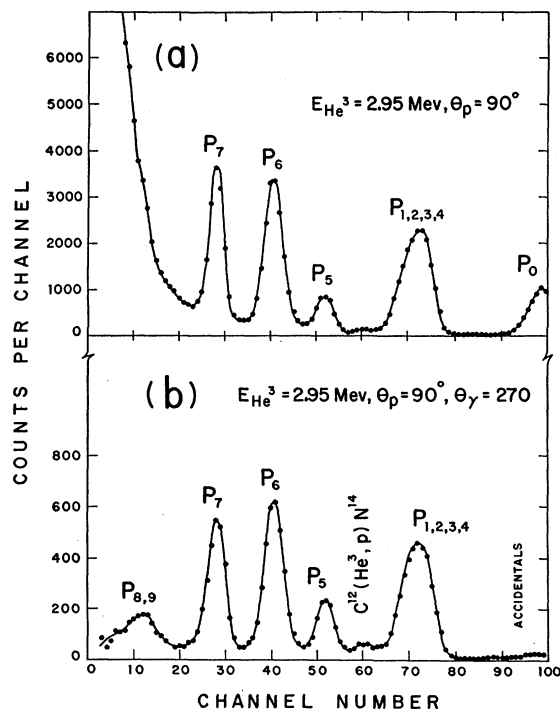


FIG. 1. Proton energy spectra from  $O^{16}(He^3,p)F^{18}$  obtained using a CsI crystal to detect protons emerging at  $90^\circ$  to the direction of a 2.95-Mev  $He^3$  beam. (a) is a direct spectrum while (b) is measured in coincidence with all gamma rays with energy greater than 700 kev ( $\theta_\gamma = 270^\circ$ ). The label  $P_i$  refers to the proton group feeding the  $i$ th excited level of  $F^{18}$ .

<sup>21</sup> D. A. Bromley, J. A. Kuehner, and E. Almqvist, Nuclear Phys. **13**, 1 (1959).

<sup>22</sup> D. A. Bromley, E. Almqvist, H. E. Gove, A. E. Litherland, E. B. Paul, and A. J. Ferguson, Phys. Rev. **105**, 957 (1957).

<sup>23</sup> C. W. Snyder, S. Rubin, W. A. Fowler, and C. C. Lauritsen, Rev. Sci. Instr. **21**, 852 (1950).

<sup>24</sup> A. E. Litherland, E. B. Paul, G. A. Bartholomew, and H. E. Gove, Phys. Rev. **102**, 208 (1956).

<sup>25</sup> R. L. Clarke, Nuclear Instr. **3**, 233 (1958).

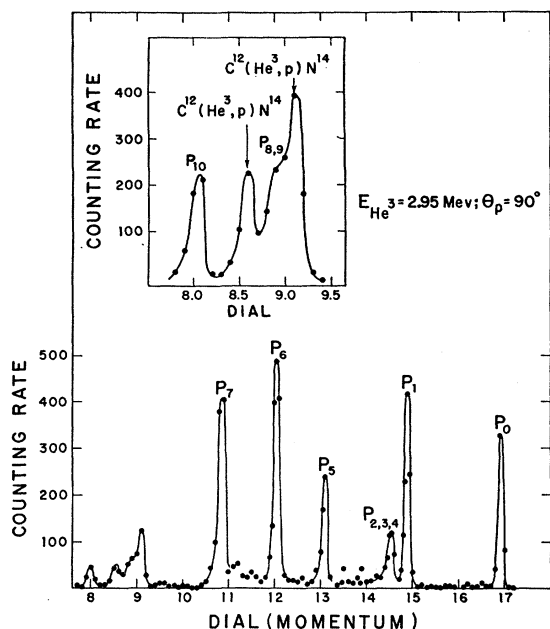


FIG. 2. Proton energy spectrum from  $O^{16}(He^3,p)F^{18}$  obtained in a Kellogg-type  $180^\circ$  magnetic spectrometer set for a resolution of  $\sim 1\%$  in momentum. The detection angle and incident energy used are indicated. The inset spectrum shows the region from  $P_8$ – $P_{10}$  with greater expansion.

resolution of  $\sim 1\%$  in momentum. The detection angle and incident beam energy are the same as above. The inset spectrum shows the low-energy region with greater expansion. There are two proton groups from the contaminant reactions  $C^{12}(He^3,p)N^{14*}$  (5.69 Mev) and (5.83 Mev) which tend to obscure the region near  $P_8$  and  $P_9$ ; however, repeated measurements using first an  $Al_2O_3$  target and second a carbon target have allowed the contaminant identification to be made. Although in this measurement there is no evidence for more than a single group, a doublet, corresponding to  $P_8$  and  $P_9$ , has been reported in this energy region.<sup>7-9</sup> The fact that the excitation energy in  $F^{18}$  obtained from this measurement for the unresolved doublet, 3.14 Mev, corresponds well with one member of the pair of levels reported and not with the other (Fig. 12 contains the most recent energy values) suggests that  $P_9$  is fed more strongly than  $P_8$  at this angle and energy.

The spectra in Fig. 3 were obtained using the magnetic analyzer set for a resolution of  $\sim 0.25\%$  in momentum and using an  $Al_2O_3$  target of 250 Å. These spectra show peaks corresponding to four levels in  $F^{18}$  in the region of 1 Mev. The marked dependence of the intensities of these groups on the angle of detection and on the incident energy made it possible to choose conditions such that a selected group was enhanced relative to its neighbors. This feature permitted the selection of particular groups for coincidence studies using high-efficiency scintillation detectors which other-

wise could not resolve closely spaced groups. These measurements will be reported later in this paper.

## 2. Yield Curves

Figure 4 shows the  $90^\circ$  excitation functions for the various proton groups as well as for the alpha-particle group to the ground state of  $O^{15}$ . In these measurements the Frisch-gridded ionization chamber was used. A typical spectrum obtained with this instrument is shown in Fig. 5. Marked resonance structure is observed corresponding to excitations of the compound nucleus,  $Ne^{19}$ , of  $\sim 11$  Mev. Figure 6 shows the proton angular distributions for the groups  $P_0$ ,  $P_5$ , and the unresolved groups  $P_{1,2,3,4}$  for an incident energy of 2.425 Mev, corresponding to the first peak in the excitation curve.

It is possible, using compound nucleus formalism, to make a detailed fit to the alpha-particle differential cross sections over the region near 2.4 Mev assuming two interfering resonances with spins of  $\frac{1}{2}$  and  $\frac{5}{2}$ , respectively, and like parity.<sup>21</sup> Unfortunately, any similar attempt at fitting the proton excitation curves or angular distributions for the case of nonzero spin final state is rendered impractical due to the introduction of new parameters in addition to those involved in the case of alpha particles. It is to be noted, as well, that the presence of odd terms in the proton angular dis-

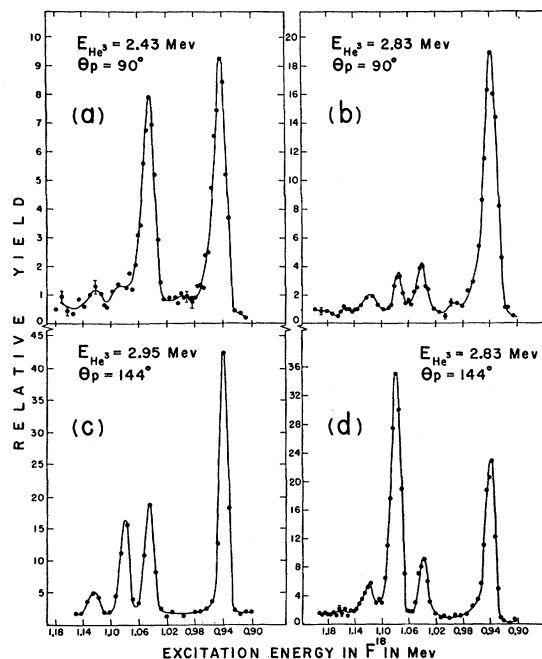


FIG. 3. Proton energy spectra from  $O^{16}(He^3,p)F^{18}$  obtained in a Kellogg-type  $180^\circ$  magnetic spectrometer. The spectrometer was set for a resolution of  $\sim 0.25\%$  in momentum. An  $Al_2O_3$  target of thickness 250 Å was used. The abscissa gives the corresponding excitation in  $F^{18}$ . The angle of observation with respect to the  $He^3$  beam and the incident  $He^3$  energy are inset for each spectrum.

tributions demonstrates the presence in these cases of interference between compound nucleus states of opposite parity. Similarly, attempts at analysis of  $He^3, p\gamma$  angular correlations are frustrated by the large number of unknowns.

### 3. De-Excitation Branching Ratios

In order to study the gamma-ray de-excitation of each of the  $F^{18}$  levels,  $p\gamma$  coincidence measurements were made using high-efficiency CsI counters with pulse-height selection to identify particular states. In some cases, such as for the group of levels near 1-Mev excitation which could not be resolved by these detectors, it was possible to choose a bombarding energy and angle that favored a selected state as discussed in Sec. C1.

The states for which detailed de-excitation studies have been made are shown in Fig. 7. In the discussion that follows, the levels are identified by the excitation energies shown here.

Figure 8 shows spectra of gamma radiation which is coincident with protons leading to the  $F^{18}$  level at 1.70 Mev. The de-excitation branching ratio for this level is obtained directly from the relative intensities of the various radiations. The three geometrical arrangements shown in the figure were used to average over angular correlation effects. In the analysis, after correcting the observed intensity of the different lines for the relative counter efficiencies, the angular correlations in both

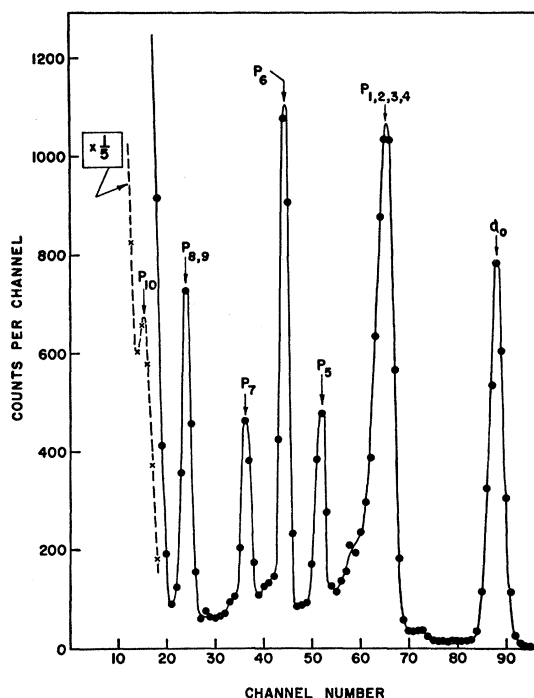


FIG. 5. Typical particle spectrum obtained using a Frisch-gridded ionization chamber to detect particles at  $90^\circ$  to the incident 3.1-Mev  $He^3$  beam. The chamber gas pressure used was 30 psi. At this particular pressure the range of the ground-state proton group exceeds the effective length of the chamber and the corresponding peak is folded back under the  $P_{1,2,3,4}$  peak.

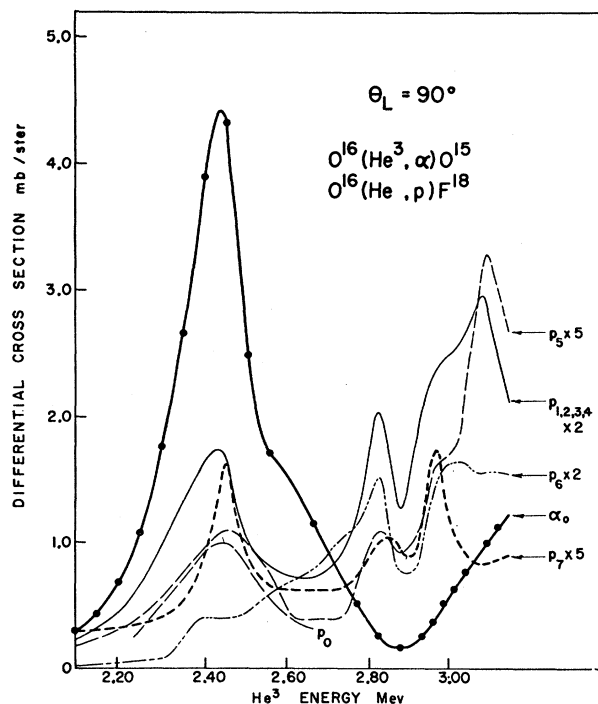


FIG. 4. Excitation curves for alpha particles and protons from the  $O^{16} + He^3$  reactions measured at  $90^\circ$  to the incident beam.

$\theta$  and  $\phi$  planes were fitted to a two-term expansion in even Legendre polynomials. This procedure, while sampling only three points in the angular correlation, is not expected to introduce a large error because the correlation coefficients were deliberately attenuated by use of large detector solid angles. This solid angle was  $\sim 0.25$  steradian.

A peak at 1.70 Mev corresponding to a ground-state transition is seen, as well as peaks corresponding to a

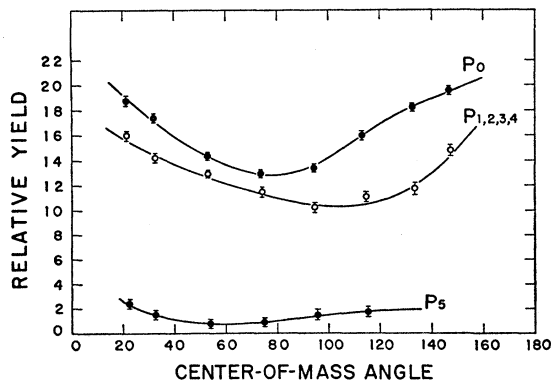


FIG. 6. Angular distributions of proton groups from the  $O^{16}(He^3, p)F^{18}$  reaction for an incident  $He^3$  energy of 2.425 Mev. These have been converted to center-of-mass angles and intensities.

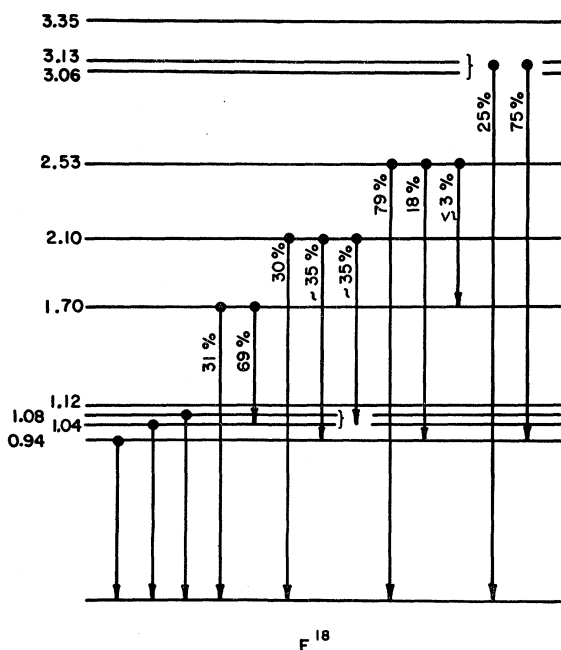


FIG. 7. Gamma-ray de-excitation branching ratio measurements are summarized in the level diagram. The relative de-excitation probabilities are expressed as percentages of the total number of de-excitations.

cascade through the level at 1.04 Mev. The relative de-excitation probabilities are expressed on the inset level diagram as percentages of the total number of de-excitations.

Figures 9 and 10 show spectra of radiation coincident with protons leading to the next higher level in  $F^{18}$ , at 2.10 Mev. The spectrum in Fig. 9 contains a peak corresponding to a ground-state transition as well as a wide peak corresponding to several gamma-ray transi-

tions of about one-Mev energy. The spectrum in Fig. 10 shows the region of one Mev with more expansion. The data are those from several coincidence runs measured using different counter angles. It is obvious from the width of the peak and from the energies of the transitions involved that the cascade  $2.10 \rightarrow 0.94 \rightarrow$  g.s. is present. The data were subjected to a computer curve fitting program<sup>26</sup> in which both the energies and the intensities of four gamma-ray components were adjusted for best fit. The results of this analysis are included in tabular form in Fig. 10. The curve corresponding to this fit is shown in the figure. The analysis confirms the presence of a cascade through the 0.94-Mev state and suggests one and perhaps two additional cascades involving either or both of the levels at 1.04 and 1.08 Mev. Unfortunately, the resolution available was not sufficient to distinguish between these alternatives.

Figure 11 shows gamma rays in coincidence with the proton group leading to the excited level at 2.53 Mev. There is a strong ground-state de-excitation branch and a weaker branch to the 0.94-Mev level. A possible transition to the level at 1.70 Mev of  $<3\%$  is suggested by indications of peaks at 0.66, 0.83, and 1.04 Mev.

The measurement of the gamma-ray de-excitation branching ratio of the unresolved levels near 3.1 Mev was made considerably more difficult as a result of the presence of proton groups from the contaminant reactions  $C^{12}(He^3, p)N^{14*}$  (5.69 Mev) and (5.83 Mev). As a result of the carbon target contamination, careful measurements were necessary, using both  $Al_2O_3$  and C targets, in order to remove the contribution due to the contaminant.

It cannot be stated with certainty that the level at 3.06 Mev is not contributing to the coincidence counting

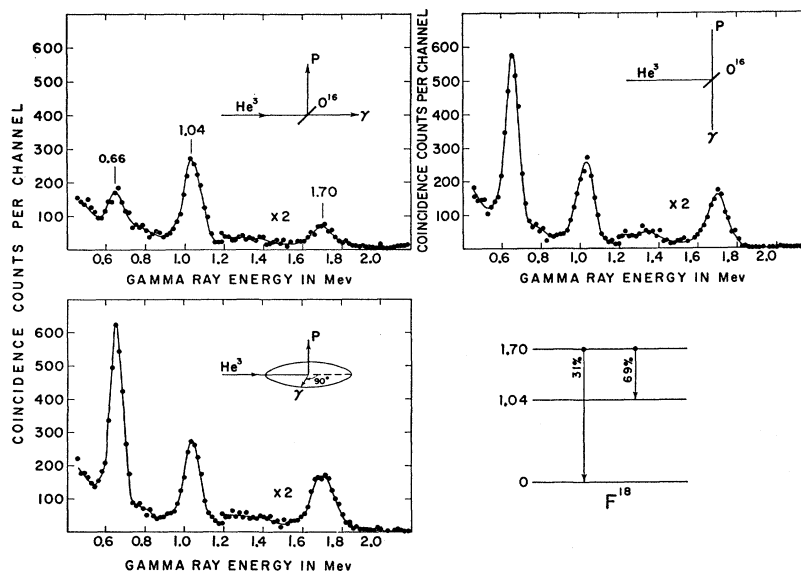


FIG. 8. Spectra of gamma radiation coincident with protons leading to the  $F^{18}$  level at 1.70 Mev; the spectra have been normalized to the same number of protons. The geometries used are indicated for each spectrum. The relative de-excitation probabilities are expressed on the inset level diagram as percentages of the total number of de-excitations.

<sup>26</sup> A. J. Ferguson (private communication).

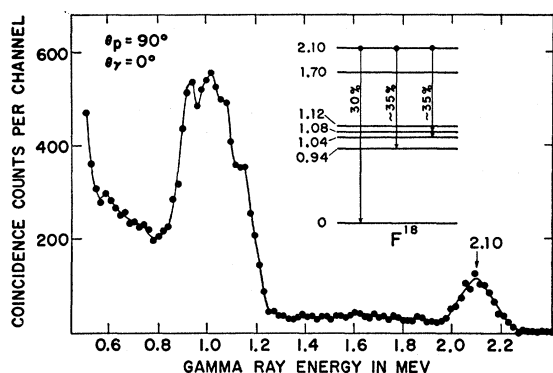


FIG. 9. Spectrum of radiations coincident with protons leading to the  $F^{18}$  level at 2.10 Mev. The relative de-excitation probabilities are given on the inset level diagram.

rate. The magnetic analyzer runs (measured for the same energy and angle as was employed for the coincidence runs described here) show that the level at 3.13 Mev is being fed and are consistent with a somewhat weaker feeding of the level at 3.06 Mev.

Figure 12(a) shows the coincidence spectra obtained with the above two targets and Fig. 12(b) shows the difference spectrum. A strong de-excitation to the level at 0.94 Mev is observed as well as a weaker transition to the ground state.

Measurements also were made to elucidate the modes of de-excitation of the four levels near 1 Mev. Since the CsI spectrometer could not resolve the corresponding proton groups, bombarding energies and observation angles for the protons were chosen (by referring to Fig. 3) such that only the 0.94- and 1.04- or the 0.94- and 1.08-Mev levels were being fed with appreciable probability. Coincident gamma radiation spectra

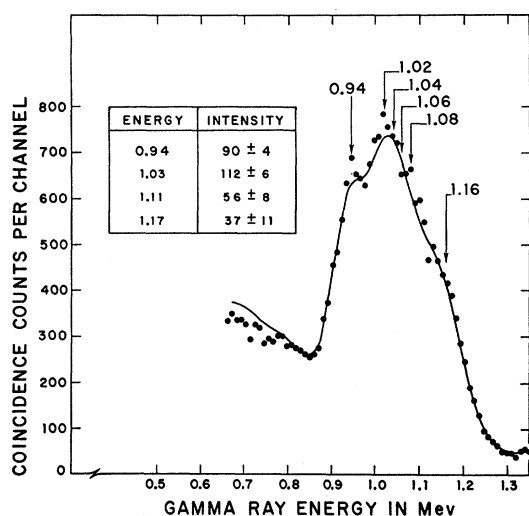


FIG. 10. Spectrum of radiation coincident with protons leading to the  $F^{18}$  level at 2.10 Mev, showing the pulse-height region near 1 Mev with large expansion. The inset table lists the energies and relative intensities obtained in a computer curve fitting analysis of the spectrum into four components.

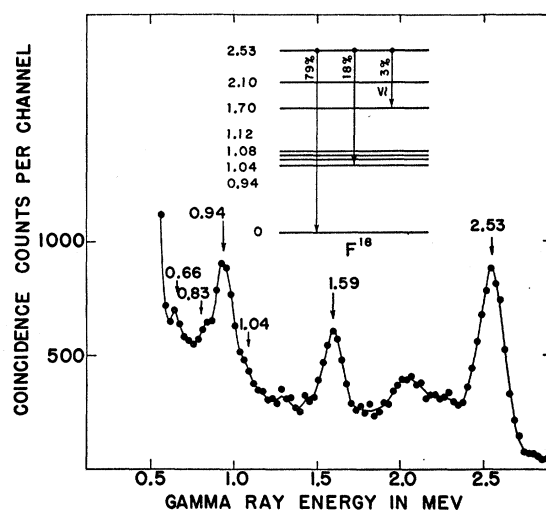


FIG. 11. Spectrum of radiation coincident with protons leading to the  $F^{18}$  level at 2.53 Mev. The relative de-excitation probabilities are given on the inset level diagram.

measured under these conditions (see Figs. 13 and 14) indicate that the levels at 0.94, 1.04, and 1.08 Mev have ground-state transitions but that the level at 1.12 Mev does not.

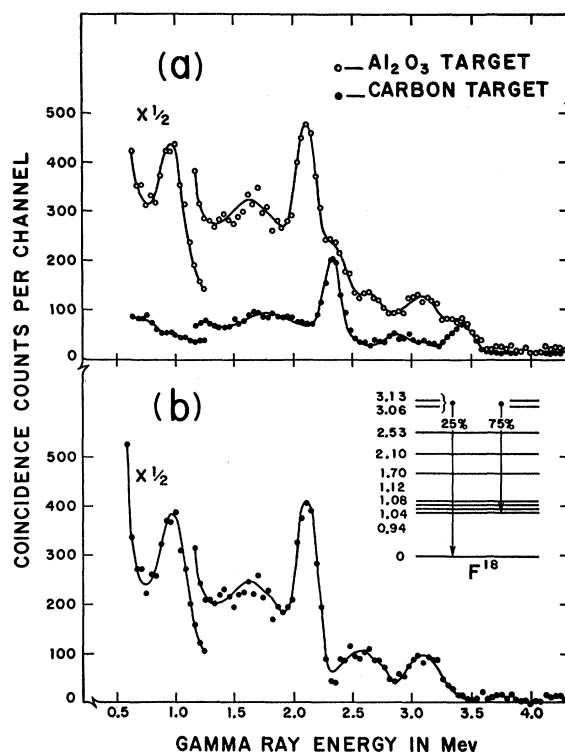


FIG. 12. Spectra of radiation coincident with the unresolved group of protons leading to the  $F^{18}$  levels at 3.06 and 3.13 Mev. The protons were detected at  $90^\circ$  to a 2.95-Mev  $He^3$  beam. (a) shows coincidence spectra obtained using  $Al_2O_3$  and carbon targets while (b) shows the difference between the two spectra of (a). The relative de-excitation probabilities are given on the inset level diagram.

The results of the gamma-ray de-excitation branching ratio measurements are summarized in the level diagram of Fig. 7.

#### 4. Angular Correlations

As mentioned above, the large number of parameters which enter the correlation formalism preclude detailed analysis of angular correlations in this reaction. However, it is possible to use the results of angular correlation measurements, in the cases where anisotropies occur, to preclude zero spin for the  $F^{18}$  levels involved.

An inspection of Fig. 8, which shows spectra of radiation in coincidence with  $P_5$  for three different geometrical arrangements, reveals that both the 1.70- and 0.66-Mev gamma radiations are markedly anisotropic. Thus, the  $F^{18}$  level at 1.70 Mev cannot have zero spin. On the other hand, the radiation of 1.04 Mev appears to be isotropic (to within 5%) in agreement with its assignment as the  $0^+$ ,  $T=1$  analog of the  $O^{18}$  ground state.

Similarly, the gamma radiation of 2.10 Mev in coincidence with the proton group  $P_6$  is anisotropic, as are the gamma radiations of 2.53 Mev coincident with  $P_7$  and  $\sim 2.1$  Mev coincident with one or both of  $P_8$

and  $P_9$ . Thus, both of the  $F^{18}$  states at 2.10, 2.53 and at least one of the doublet at  $\sim 3.1$  Mev have  $J > 0$ .

In attempting to gain more information regarding the  $F^{18}$  states at 0.94, 1.04, and 1.08 Mev, the angular correlations shown in Figs. 13 and 14 were measured. In order to use the CsI detector, which cannot resolve the proton groups to these states, detection angles and  $He^3$  energies were again chosen such that either the 0.94- and 1.04-Mev levels or the 0.94- and 1.08-Mev levels were being fed most strongly. The conditions used in the measurements are those used in the magnetic analyzer runs of Figs. 3(a) and 3(d), respectively. In both cases the 0.94-Mev radiation is strongly anisotropic, ruling out spin zero for the  $F^{18}$  level of that energy; a possible  $P_4(\cos\theta)$  term in the correlation shown in Fig. 14 suggests  $J > 1$  and the presence of  $E2$  in the gamma radiation. Furthermore, in each case the other radiation (1.04 and 1.08 Mev, respectively) is isotropic within the accuracy of the experiment.

Direct angular distributions were measured for the radiation from the states near 1 Mev. Again, within the accuracy of the measurements, the composite peak corresponding to the sum of the 1.04- and 1.08-Mev radiations showed isotropy while that of the 0.94-Mev radiation did not.

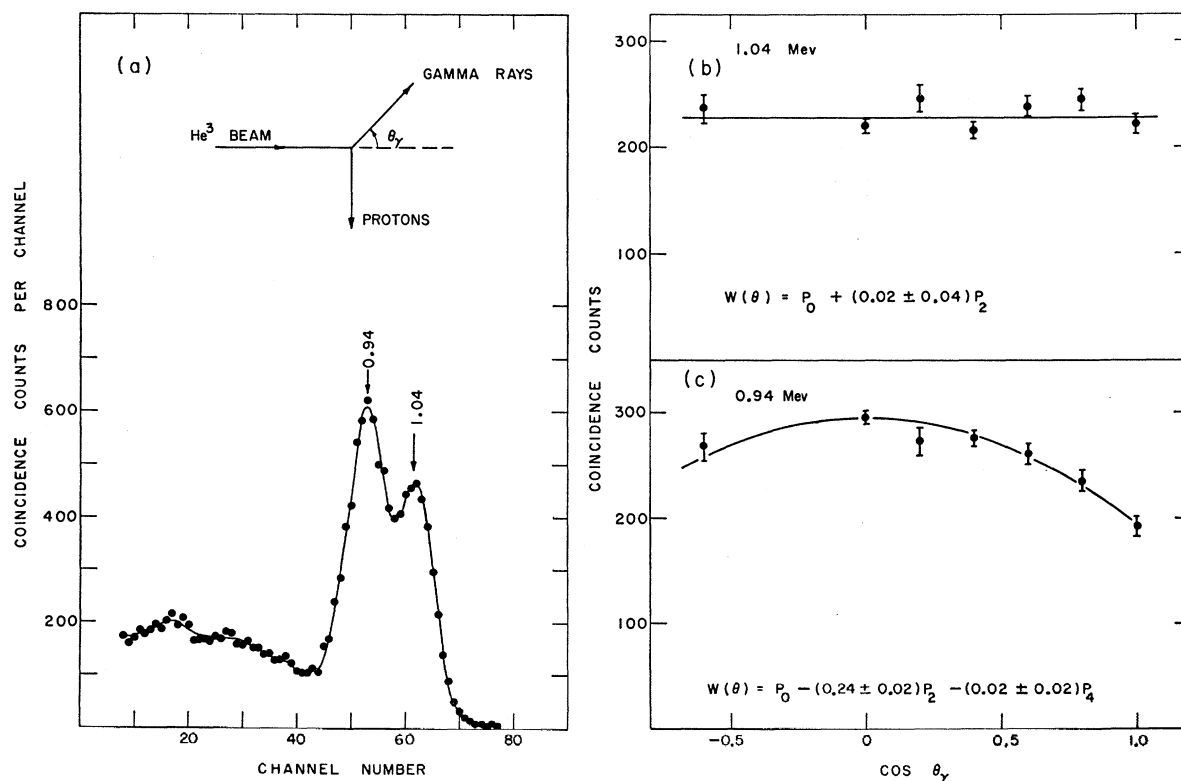


FIG. 13. Angular correlations in the reaction  $O^{16}(He^3,p)F^{18}$ . (a) shows a typical spectrum of radiation coincident with the unresolved proton group  $P_{1,2,3,4}$ , for  $E_d=2.43$  Mev and  $\theta_p=90^\circ$ . (b) and (c) are the angular correlations of the 1.04-Mev and 0.94-Mev radiations, respectively, measured in the geometry shown inset in (a). The least-squares angular correlation functions are included.

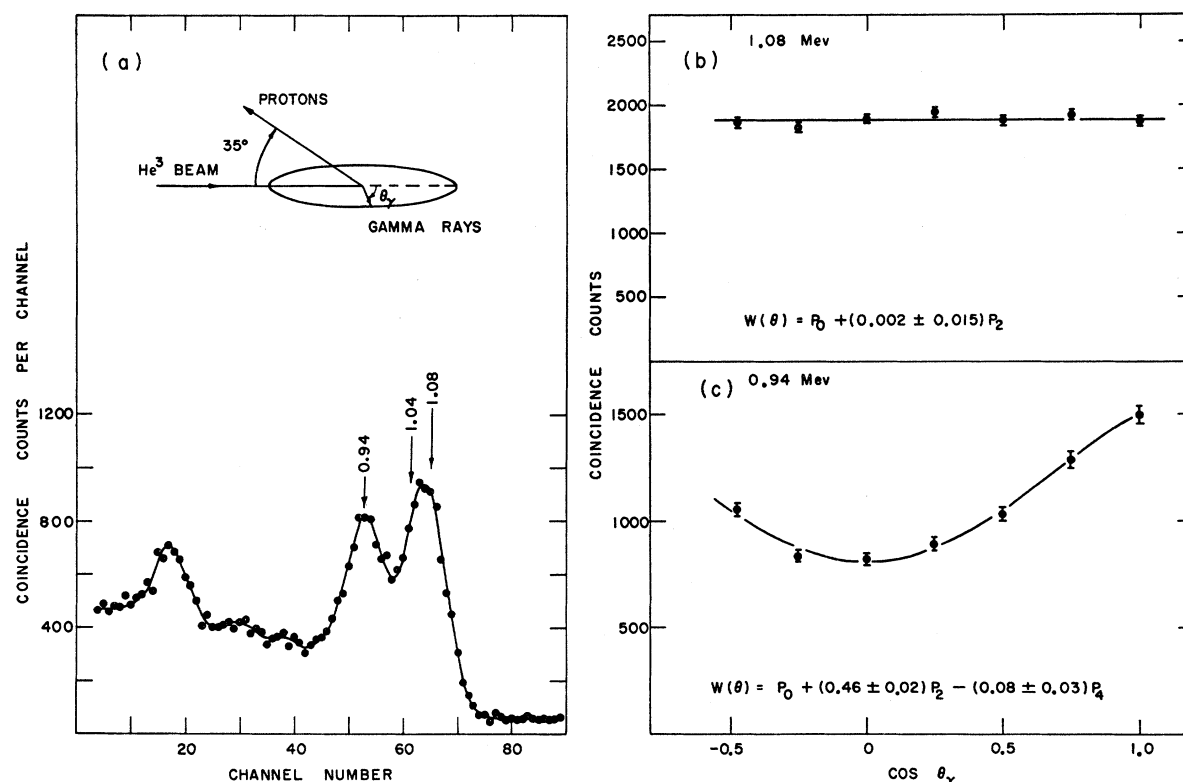


FIG. 14. Angular correlations in the reaction  $O^{16}(He^3, p\gamma)F^{18}$ . (a) shows a typical spectrum of radiation coincident with the unresolved proton group  $P_{1,2,3,4}$  for  $E_d=2.83$  Mev and  $\theta_p=145^\circ$ . (b) and (c) are the angular correlations of the 1.08-Mev and 0.94-Mev radiations, respectively, measured in the geometry shown inset in (a). The least-squares angular correlation functions are included.

These data suggest, but do not prove, that the F<sup>18</sup> levels at 1.04 and 1.08 Mev each have zero spin.

Since the gamma-ray transitions reported herein have all been observed in coincidence with protons feeding the levels and with the expected coincidence efficiency, it can be concluded that they all have lifetimes of magnitude less than roughly the coincidence resolving time. The coincidence resolving time used was  $\tau=2 \times 10^{-8}$  second. A more careful examination of the lifetime of the state at 0.94 Mev, using a delayed-coincidence technique, has led to a limit of less than  $5 \times 10^{-9}$  second for this state.

#### D. DISCUSSION

##### 1. Level Assignments

As yet, firm spin and parity assignments cannot be made to all of the low-lying F<sup>18</sup> levels. However, the assignments to certain of the levels are fixed and to others are suggested.

The systematics of odd-odd nuclei together with the allowed nature of the F<sup>18</sup> beta decay<sup>27</sup> suggest an assignment of  $1+$  for the F<sup>18</sup> ground state.

Observation<sup>14,15</sup> of a 1.04-Mev gamma ray and none of energy 1.08 Mev following the beta decay of Ne<sup>18</sup>,

<sup>27</sup> F. Aijzenberg-Selove and T. Lauritsen, Nuclear Phys. 11, 1 (1959).

makes it almost certain that the level at 1.04-Mev excitation in F<sup>18</sup> is the  $0+ T=1$  analog of the O<sup>18</sup> ground state. This level would be expected to be fed by the beta decay considerably more strongly than that at 1.08 Mev since it would involve a superallowed  $0 \rightarrow 0$  transition. This identification is corroborated by studies<sup>18,19</sup> which show identical angular distributions for O<sup>16</sup>(He<sup>3</sup>, p)F<sup>18\*</sup> (1.04 Mev) and O<sup>16</sup>(t, p)O<sup>18</sup> (ground state) but quite different results for O<sup>16</sup>(He<sup>3</sup>, p)F<sup>18\*</sup> (1.08 Mev) which is fed only extremely weakly. The identification of the 1.04-Mev state as the  $0+ T=1$  analog of the O<sup>18</sup> ground state is, of course, consistent with the observed isotropy of the de-excitation radiation from this level in the present investigation. The  $T=1$  assignment to the 1.04-Mev level also leads to the expectation that its formation should be inhibited in the reaction Ne<sup>20</sup>(d, α)F<sup>18</sup> if isotopic spin is conserved. Measurements made by Freeman<sup>9</sup> suggest on this basis  $T=1$  assignments to levels at 1.04 Mev and 4.74 Mev, and also possibly to levels at 3.06 Mev and 4.63 Mev.

The levels at 0.94 Mev and 1.12 Mev, together with the ground state, very likely form the  $1+$ ,  $3+$ ,  $5+$  sequence predicted by both Elliott and Flowers<sup>3</sup> and by Redlich.<sup>4</sup> The lifetime of the 0.94-Mev state against decay to the ground state has been shown by the coincidence measurements reported herein and by similar



TABLE I. Comparison of the experimental relative widths (expressed in all cases as a percentage of the total de-excitation) with those obtained from the Weisskopf extreme single-particle model modified to include isotopic spin inhibition of  $M1$  and  $E1$  transitions and collective enhancement of  $E2$  transitions. For levels where the spin and parity have not been uniquely determined, the values suggested by the intermediate-coupling shell-model calculations have been used (see Fig. 16 for the level identifications).

Initial state (Mev)	Final state (Mev)	Multipole character	Relative de-excitation branching	
			Calculated	Experiment
1.70 1+, $T=0$	g.s.	$M1^a$	14	31
	0.94	$E2^b$	0.1	Not observed
	1.04	$M1$	83	69
	1.08	$E1^c$	2.5	Not observed
2.10 (2+) $T=0$	g.s.	$M1^a$	84	30
	0.94	$M1^a$	14	$\sim 35$
	1.04	$E2^b$	2	$\sim 35$
	1.08	$M2$	0.01	$\sim 35$
2.53 (3+) $T=0$	g.s.	$E2^b$	78	79
	0.94	$M1^a$	18	18
	1.12	$E2^b$	4	Not observed
	1.70	$E2^b$	0.3	$\leq 3$
3.06–3.13 (2+, $T=1$ )	g.s.	$M1$	71	25
	0.94	$M1$	23	75
	1.70	$M1$	6	Not observed

<sup>a</sup> Inhibited  $\Delta T=0$   $M1$  transition (factor of 120 inhibition included).

<sup>b</sup> Enhanced  $E2$  transition (factor of 5 enhancement included).

<sup>c</sup> Inhibited  $\Delta T=0$   $E1$  transition (factor of  $10^3$  inhibition included).

measurements of Allen *et al.*<sup>16</sup> to be less than  $5 \times 10^{-9}$  sec, while the absence of a Doppler shift in  $H^3(O^{16}, p)O^{18}$  places a lower limit of  $4 \times 10^{-12}$  sec on the lifetime.<sup>28</sup> The linear polarization of the 0.94-Mev transition<sup>29</sup> requires that the 0.94-Mev state has positive parity. This limitation and the limits set on the lifetime require the transition to be either  $M1$  or  $E2$ , both of which give  $\tau \sim 10^{-11}$  sec because of the  $M1$  selection rule operative in  $\Delta T=0$  transitions<sup>30</sup> and the collective enhancement<sup>31</sup> of  $E2$  transitions. Measurements of Allen *et al.*,<sup>16</sup> using the  $O^{16}(He^3, p\gamma)F^{18}$  reaction, show that the 1.12-Mev level decays by a cascade transition through the 0.94-Mev level. The measured lifetime of  $\sim 2 \times 10^{-7}$  sec is in excellent accord with that calculated by Elliott for an  $E2$  transition between these two states if they are identified with the 3+ and 5+ levels of the sequence. Additional evidence, suggesting an  $E2$  nature for this transition, is obtained from a measurement of the internal conversion coefficient<sup>17</sup> for this radiation.

The observed anisotropies in the angular correlation of the radiation from the state at 1.70 Mev in  $F^{18}$  reported herein, together with the  $l=0$  angular momentum transfer observed in forming this state in

either the  $F^{19}(p, d)F^{18}$  reaction<sup>10</sup> or the  $F^{19}(d, t)F^{18}$  reaction,<sup>12</sup> fix the assignment to the state in  $F^{18}$  at 1.70 Mev as 1+.

No specific assignments are as yet possible for the levels at 2.10, 2.53, and the doublet at  $\sim 3.1$  Mev.  $J=0$  can be ruled out for all of these states because of the anisotropic angular correlations observed in the  $O^{16}(He^3, p\gamma)F^{18}$  measurements reported herein. As well, rough upper limits on the spins can be set by noting that all of these states show transitions to the 1+ ground state with lifetimes shorter than the coincidence resolving time,  $\tau \sim 2 \times 10^{-8}$  sec, used in the  $p\gamma$  coincidence measurements. These considerations lead to the limit of  $J \leq 3$  for each of these states. The absence of transitions from the 2.53- and  $\sim 3.1$ -Mev states to the  $J=0$  states at 1.04 and 1.08 Mev (discussed below) is in accord with  $J > 0$  and suggests  $J > 1$  for these cases.

This completes a consideration of all of the levels studied in this investigation except that at 1.08 Mev. This level appears to represent an anomalous situation, there being no counterpart in the theoretical predictions. Early measurements with the  $N^{14}(\alpha\gamma)F^{18}$  reaction<sup>32</sup> first showed the strong gamma-ray transitions which suggested the existence of a level in  $F^{18}$  at this energy. More recent measurements<sup>33</sup> carried out in this laboratory, using this same reaction, established that the strong transitions were between a resonance level at 5.60-Mev excitation and the levels at 3.06 and 1.08 Mev. Since the measured angular correlations are in complete accord with a  $J=1$  assignment to the level at 5.60 Mev and  $J=0$  to that at 1.08 Mev, an attractive explanation of the two strong transitions observed was that they were uninhibited  $\Delta T=1$  transitions to  $T=1$  states. However, in the face of overwhelming evidence from other sources discussed above, it appears that it is not the 1.08-Mev level but rather the level at 1.04 Mev which has  $T=1$ . Thus, neither the level at 1.08 nor possibly the level at 3.06 Mev have  $T=1$ , as was earlier believed.

It is possible that the level at 1.08 Mev may have negative parity, and thus would not be considered in the theoretical treatments<sup>3,4</sup> made to date.

The values or limits thereto of the spins and parities of the levels of  $F^{18}$  discussed in this section are summarized in column A of Fig. 15.

## 2. Branching Ratios

The experimentally determined de-excitation branching of the  $F^{18}$  levels is summarized in Fig. 7. This section compares these values with modified single-particle estimates, based on the identifications with the theoretical predictions shown in Fig. 16. These identifications are not all definite but appear to be the most reasonable choices. Table I contains the experimental

<sup>28</sup> A. E. Litherland, B. M. Adams, D. Eccleshall, and M. J. L. Yates, *Proceedings of the Kingston Conference on Nuclear Structure*, edited by D. A. Bromley and E. W. Vogt (University of Toronto Press, Toronto, 1960).

<sup>29</sup> A. E. Litherland and H. E. Gove, *Bull. Am. Phys. Soc.* **3**, 200 (1958).

<sup>30</sup> G. Morpurgo, *Phys. Rev.* **110**, 721 (1958); E. K. Warburton, *Phys. Rev.* **113**, 595 (1959).

<sup>31</sup> F. C. Barker, *Phil. Mag.* **1**, 329 (1956).

<sup>32</sup> P. C. Price, *Proc. Phys. Soc. (London)* **A68**, 553 (1955).

<sup>33</sup> E. Almqvist, D. A. Bromley, and J. A. Kuehner, *Bull. Am. Phys. Soc.* **3**, 27 (1958).



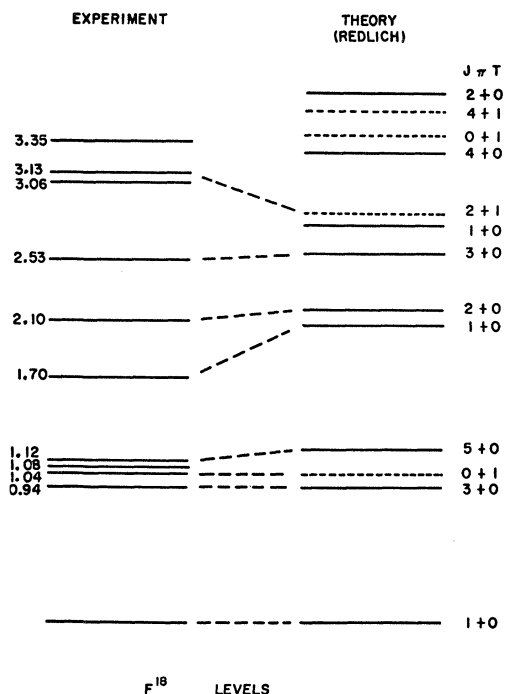


FIG. 16. The observed excitations of levels in  $F^{18}$  are compared with the intermediate-shell-model predictions of Redlich, modified by a scale factor of 0.6 and with the  $T=1$  band (dotted) adjusted relative to the  $T=0$  band (solid) to fit the 1.04-Mev separations observed in  $F^{18}$ . The dashed lines indicate the level identifications used in the comparisons of Table I.

excitations of these bands depends strongly upon the exchange character of the nuclear potential assumed<sup>3</sup> and is not expected to be accurately given by the model.

Elliott and Flowers used a Rosenfeld exchange potential of Yukawa shape for the interaction between pairs of particles outside the  $O^{16}$  core. The separation of single-nucleon  $s$  and  $d$  levels, as well as the spin-orbit force, was determined from the level structure of  $O^{17}$ . Intermediate values of coupling between  $jj$  and  $LS$  limits were obtained by varying the depth  $V_c$  of the central potential. The range  $40 < V_c < 50$  Mev is displayed here since this gives a reasonable value for the deuteron binding energy and gives satisfactory agreement for mass-16<sup>37,38</sup> and mass-19<sup>39</sup> nuclei.

Redlich used a Serber exchange potential of Gaussian shape for the internucleon interaction and chose parameters to fit  $n$ - $p$  triplet scattering and the deuteron binding energy. Again the spin-orbit force and  $s$ - $d$  splitting was determined from the level structure of  $O^{17}$ .

It should be noted that both the Elliott and Flowers calculations and the Redlich calculations give the same level sequence for the  $T=0$  and  $T=1$  levels considered

separately. In either case the predicted  $T=0$  spectra are characterized by the low-lying 1, 3, 5 positive-parity sequence followed by a relatively large gap in which no  $T=0$  states are predicted. This same sequence followed by a gap can be recognized in the experimental spectrum.

For the case of the Redlich predictions it is found that if a scale factor of 0.6 is arbitrarily applied to bring the first predicted  $J=3$ ,  $T=0$  level to 0.94 Mev, the resultant spectrum provides a not unreasonable description of the states observed. The level excitations obtained in this way are compared in Fig. 16 with the experimentally observed excitations. The level identifications used in Table I are indicated by the dashed lines. It is of interest to note that also in the  $O^{16}$  calculations of Elliott and Flowers<sup>37</sup> a similar multiplicative factor, 0.85, is required to obtain agreement with the observed spectrum.<sup>38</sup> It remains to be seen whether the detailed theory can be altered in such a way as to fit the observed energy spacings. It has been pointed out by Elliott<sup>40</sup> in this connection that the effect of surface particle coupling similar to that required to explain the lifetime<sup>3</sup> of the 197-kev  $E2$  transition in  $F^{19}$  has a large effect on level spacings in the mass-18 nuclei although the corresponding effect on the mass-19 system is small. It should be noted that the intermediate-coupling shell-model predictions were made before any accurate experimental data for mass-18 nuclei were available to guide the choice of parameters, and it may well be that details of the calculations can be altered to obtain better agreement with observed level spacings. As yet there are not available any calculated transition widths to compare with the measured  $\gamma$ -ray branching ratios.

It is apparent from Fig. 15 that if one omits the 1.08-Mev state, then the sequence of spins predicted by the model is in accord with the measured values or limits. One would normally argue that additional states beyond those predicted by these calculations are the result of core excitation. It would be expected *a priori* that one or more of such states with negative parity, corresponding to single-particle core excitation, should appear at relatively low excitations and that positive-parity states characteristic of two-nucleon core excitation should not appear below about 6 Mev. These considerations suggest a negative-parity assignment to the state at 1.08 Mev. It is noted that similar low-lying negative-parity states are known to exist<sup>27</sup> in  $F^{19}$ .

In view of the recent attempts to use the nuclear cluster model<sup>41</sup> to correlate spectroscopic information in light nuclei, it may be of interest to note that the 1.08-Mev state and that at 3.06 Mev are both fed very strongly<sup>32,33</sup> in the  $N^{14}(\alpha, \gamma)F^{18*}$  reaction. The very large widths of these transitions suggest some connection

<sup>37</sup> J. P. Elliott and B. H. Flowers, Proc. Roy. Soc. (London) **A242**, 57 (1957).

<sup>38</sup> D. A. Bromley, H. E. Gove, J. A. Kuehner, A. E. Litherland, and E. Almqvist, Phys. Rev. **114**, 758 (1959).

<sup>39</sup> E. B. Paul, Phil. Mag. **2**, 311 (1957).

<sup>40</sup> J. P. Elliott (private communication).

<sup>41</sup> K. Wildermuth and T. Kanellopoulos, Nuclear Phys. **7**, 150 (1958); **9**, 449 (1958/59). R. K. Sheline and K. Wildermuth, (to be published); G. C. Phillips and T. A. Tombrello, Nuclear Phys. (to be published).

between these states and the capturing states at 5.60 and 5.67 Mev. This would be in accord with these states involving a binary clustering of an alpha particle and  $N^{14}$  in an excited state. Similarly in  $O^{18}$  there is a state at 7.13 Mev<sup>42</sup> which is known to have a very large alpha-particle width and which shows a higher than average width for emission of  $E2$  radiation to the first excited state; in this case, of course, the associated cluster is  $C^{14}$ . On such an interpretation the  $F^{18}$  levels at 0, 0.94, and 1.12 Mev may be based on the  $N^{14}$  ground state as a parent; the  $0^+, T=1$  level at 1.04 Mev on the  $T=1$  state at 2.31 Mev in  $N^{14}$  and the level at 1.08 Mev on the  $0^-, T=0$  level in  $N^{14}$  at 4.91 Mev. In this picture the states at 6.24 and 6.65 Mev in  $F^{18}$  and those at 7.63 and 8.05 Mev in  $O^{18}$ , studied by Phillips<sup>43</sup> using the  $N^{14}(\alpha, \gamma)F^{18}$  and  $C^{14}(\alpha, \gamma)O^{18}$  reactions, respectively, would not correspond to such cluster states.

The strong-coupling collective model<sup>44</sup> has been applied with considerable success to a number of  $d$ -shell nuclei. It has permitted a simple interpretation of many of the properties of these nuclei including those of  $F^{19}$ . However, for the mass-18 system the evidence<sup>42</sup> from  $O^{18}$  argues against a strong-coupling collective-model interpretation and no detailed application of this model to  $F^{18}$  has been attempted.

$F^{18}$  probably has prolate distortion as has been suggested for  $O^{18}$  by Gove and Litherland<sup>42</sup> and which has been found to give agreement with experiment for  $F^{19}$  by Paul.<sup>39</sup> According to the Nilsson<sup>45</sup> calculations the two nucleons outside the  $O^{16}$  core on this assumption each have  $\Omega = \frac{1}{2}$  and can combine to give  $K=0$  and  $K=1$  bands. From general symmetry arguments<sup>46</sup> the low-lying rotational bands are: (a)  $T=1, K=0, J=0, 2, 4, \dots$ , (b)  $T=0, K=1, J=1, 2, 3, 4, \dots$ , and (c)  $T=0, K=0, J=1, 3, 5, \dots$ .<sup>47</sup> Although the  $K=0$

band (c) has the 1, 3, 5  $\dots$  level sequence observed for the lowest  $T=0$  levels, the calculations of Redlich<sup>4</sup> suggest that the lowest  $T=0$  levels are actually from the  $K=1$  band. The observed level sequence, however, is not that expected for band (b). These facts argue against a simple collective interpretation of the  $T=0$  levels of  $F^{18}$ .

### E. CONCLUSIONS

The de-excitation branching of the levels in  $F^{18}$  up to  $\sim 3$  Mev has been studied using  $p\gamma$  coincidence techniques. These measurements have been shown to be in reasonable agreement with tentative level identifications based on the shell-model predictions of Elliott and Flowers and of Redlich. These tentative level assignments are consistent with direct and coincidence angular correlation measurements made on the de-excitation radiation.

Acceptable agreement is found between the observed level positions and those predicted by the shell-model calculations provided (i) the  $T=1$  band of levels is arbitrarily shifted with respect to the  $T=0$  band, and (ii) a scale factor of 0.6 is arbitrarily applied to the predicted energies. The first of these is reasonable because of the extreme sensitivity of this relative shift on the exchange nature of the potential.<sup>3</sup> It remains to be seen whether detailed predictions of the energy separations can be made by reasonable changes of the potentials used.

It has not been found possible to obtain an adequate fit to the  $F^{18}$  level spectrum presented in terms of a rotational collective model. The data may, however, be qualitatively in accord with an alpha- $N^{14}$  cluster-model interpretation.

An example of the isotopic-spin selection rule inhibiting  $\Delta T=0$   $M1$  transitions in self-conjugate nuclei has been observed. The measured inhibition of 40 is in good agreement with the expectation of  $\sim 100$ .

### ACKNOWLEDGMENTS

The authors gratefully acknowledge the assistance of Dr. A. J. Ferguson in carrying out computer fitting of NaI spectra. Discussions with Dr. J. P. Elliott and Dr. T. D. Newton concerning the theoretical interpretations and with Dr. H. E. Gove and Dr. A. E. Litherland concerning the  $O^{18}$ - $F^{18}$  system are gratefully acknowledged.

<sup>42</sup> H. E. Gove and A. E. Litherland, Phys. Rev. **113**, 1078 (1959).

<sup>43</sup> W. R. Phillips, Phys. Rev. **110**, 1408 (1958).

<sup>44</sup> A. Bohr and B. R. Mottelson, Kgl. Danske Videnskab. Selskab, Mat.-fys. Medd. **27**, No. 16 (1953).

<sup>45</sup> S. G. Nilsson, Kgl. Danske Videnskab. Selskab, Mat.-fys. Medd. **29**, No. 16 (1955).

<sup>46</sup> A. K. Kerman, *Nuclear Reactions*, edited by P. M. Endt and M. Demeur (North-Holland Publishing Company, Amsterdam, 1959), p. 471.

<sup>47</sup> The corresponding statement given by Kerman,<sup>46</sup> in which the isotopic spins in bands (a) and (c) are interchanged, is in error.